J Fusion Energ
DOI 10.1007/s10894-016-0061-6

ORIGINAL RESEARCH

Temporal Variation of the Current Sheet Inductance from PACO Plasma Focus Device

M. O. Barbaglia[1] · M. Milanese[1] · L. Soto[2,3] · A. Clausse[4] · J. Moreno[2,3] · C. Pavez[2,3] · C. Moreno[5]

Abstract The temporal variation of the current sheet (CS) inductance in a plasma focus device can be calculated using the current derivative and the voltage signal acquired on the anode electrode, which are very common measurements in this type of device. The value of that inductance contains important information about the discharge performed including the CS lift-off from the insulator, voltage between the pinch extremes, maximum energy of the X-ray, energy delivered to the pinch and information about the actuating fusion mechanisms if the filling pressure is deuterium. This work discusses the values of the CS inductance extracted from several discharges of the Plasma Auto Confinado (PACO) plasma focus, installed in the National University of the Center of Buenos Aires—Argentina (2 kJ total energy, capacitor bank of 4 μF charged to 31 kV and a maximum current of 250 kA).

✉ M. O. Barbaglia
mario.barbaglia@gmail.com

[1] CONICET - Universidad Nacional del Centro de la provincia de Buenos Aires, Buenos Aires, Argentina

[2] CCHEN - Comisión Chilena de Energía Nuclear, Casilla 188-D, Santiago, Chile

[3] Departamento de Ciencias Físicas, Facultad de Ciencias Exactas, Universidad Andrés Bello, República 220, Santiago, Chile

[4] CNEA - CONICET and Universidad Nacional del Centro de la provincia de Buenos Aires, Buenos Aires, Argentina

[5] CONICET - Universidad de Buenos Aires, Buenos Aires, Argentina

Keywords Fusion · Plasma focus · Pulsed plasma

Introduction

The plasma focus devices (DPF) have been studied for five decades with the initial works of Mather [1, 2] and Filippov et al. [3]. From this starting point, multiple researchers have moved the frontier of knowledge [4–11]. These devices receive attention because they are a neutron and X-ray pulsed source of simple construction, relatively inexpensive and transportable; conditions which are very useful in technological applications [12–19].

From the beginning, the current derivative and the anode voltage signals have been the basic measurement data typically obtained by using a Rogowski coil [20] and a resistive voltage divider [21] respectively. In addition, many measurement devices are also being used to characterize and understand the behavior of DPFs. Examples of measurement methods and instruments are scintillators [22], light probing (e.g. interferometry [23]), silver activated detectors [24], proportional counters [25], radiography [26], Thomson spectrometry [27], image converters [28], pinhole cameras [29], electric and magnetic probes, among others.

In spite of the simplicity of the measures given by the current derivative and the anode voltage signals, relevant data about the plasma focus behavior can be extracted. This topic was explored by Bruzzone et al. [30] and Eltgroth [31] among others. These works deal about the methods to extract the information of current sheet inductance through time [30], the current sheet lift-off characteristic [32], the energy and voltage involved in the pinch stage and the fusion method predominant in the device [33].

Published online: 13 January 2016

Experimental Setup and Methods

The PACO plasma focus, it is currently operating at the National University of the Center of the Buenos Aires Province, Argentina. This device has a 4 cm long and 4 cm in diameter OFHC copper anode, with a cathode consisting in a solid Copper cylinder of 3.7 cm high and 7.5 cm inner diameter. The capacity of the bank is $C = 4$ μF and the parasitic inductance is $L_0 = 57$nH. The D_2 filling pressure, p_0, is in the range of few mbar. The neutron yield, Y_n, is about 2×10^8 neutrons per pulse measured with a calibrated silver activation counter. The PACO device was operated at a fixed charging voltage $V_0 = 31$ kV. A plastic scintillator type NE102 coupled to a photomultiplier was used to measure the time history of the X-ray and neutron radiation emissions placed 2.4 m from the pinch region, and at 72° measured from the anode axis. A calibrated Rogowski coil was placed in the current return path of the current sheet (CS) to measure the current time derivative, *dI/dt*, and a calibrated fast resistive voltage divider was placed on the back of the anode to determine the anode voltage drop $V(t)$. A device schematic is shown in Fig. 1.

Typical signals of *dI/dt*, $V(t)$, $I(t)$, and $L_p(t) + L_0'$ are given in Fig. 2, as an example of a shot performed at 1 mbar of D_2 filling pressure, charging the capacitor bank at 31 kV. In this figure, the time origin was labeled t_0; this is the time when the current derivative raises abruptly and coincides with the anode voltage drop. At $t = t^*$ the voltage of the capacity between the spark-gap, transmission line and the coaxial electrodes begins to raise. When the breakdown is produced, the stored energy in this, typically small, capacitor diminishes. At $t = t_1$, the CS is formed over the insulator. Later, the CS lift-off from the insulator and the axial travel begins until the end of the anode where the radial stage begins. This takes place at $t = t_2$. At $t = t_3$ the radial compression stage ends.

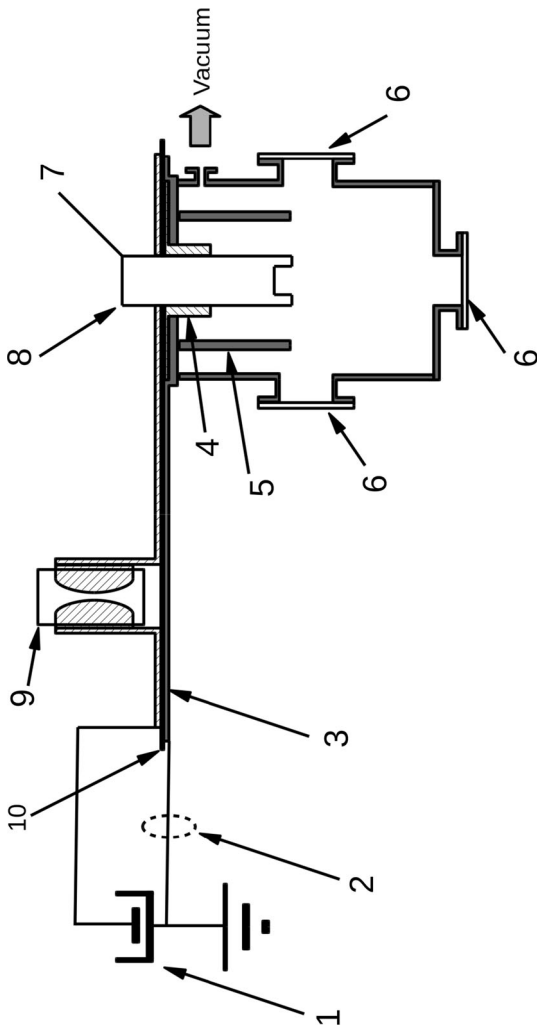

Fig. 1 Schematic diagram of PACO plasma focus device. *1* capacitor bank, *2* Rogowski coil, *3* transmission line return path, *4* insulator, *5* cathode, *6* borosilicate window, *7* voltage probe, *8* anode, *9* spark-gap and *10* transmission line insulator (Mylar)

Current Sheet Inductance, Energy Increment and Voltage in the Pinch

An equivalent circuit of the device is shown in Fig. 3. L_0' is a fixed inductance (typically small) between the voltage divider and the anode, L_p is the time varying CS inductance, *S-G* represents the spark-gap connecting the capacitor bank (C_0) to the discharge chamber, and *S-Gp* represents the closure of the circuit in the discharge chamber by the breakdown process.

From the circuit, one can write:

$$V(t) = \frac{d}{\mathrm{dt}}\left[\left(\mathrm{L}_0' + \mathrm{L}_p(t)\right)I(t)\right]$$

And hence:

$$L_p(t) + \mathrm{L}_0' = \frac{\int_{t_1}^{t} V(t)\mathrm{dt} + \left(\mathrm{L}_0' + \mathrm{L}_p(t_0)\right)I(t_0)}{I(t)}$$

In this work, the inductance was evaluated for the full set of signals and an example is shown in Fig. 2. $L_p(t) + L_0'$ is plotted because L_0' is too small to be separately determined with sufficient accuracy.The voltage drops in the pinch. $V_p(t)$ can be calculated as:

$$V_p(t) = \mathrm{V}(t) - \left[L_p(t) + \mathrm{L}_0'\right]\frac{\mathrm{dI}}{\mathrm{dt}}$$

The energy involved in the pinch $\Delta E_p(t)$ can be calculated as:

$$\Delta \mathrm{E}_p(t) = \frac{1}{2}\int_{t_2}^{t} I^2 \mathrm{dL}_p'$$

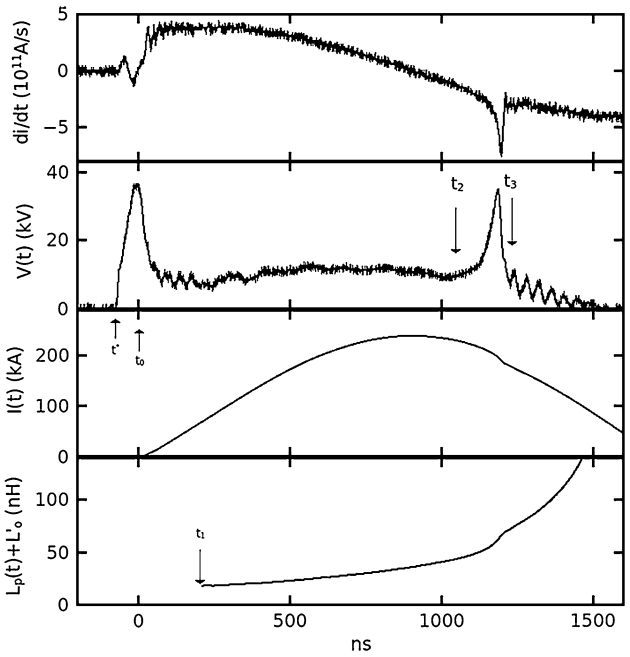

Fig. 2 Typical signals of PACO plasma-focus. From top to bottom: current derivative, anode voltage, current and current sheet inductance signal

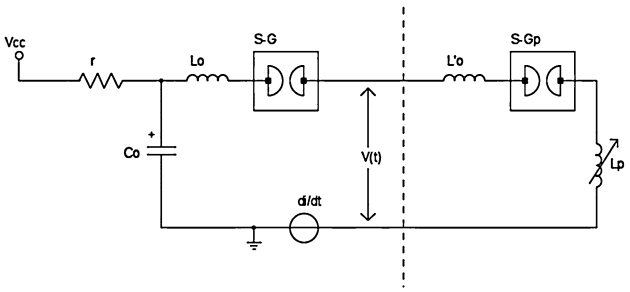

Fig. 3 Electrical diagram of the plasma focus. From the *dashed line* to the right represent the discharge chamber

Here t_2 is the instant at which the *dI/dt* dip starts, and dL'_p is the differential increase in L'_p during the pinch stage. Strictly speaking, to calculate V_p and ΔE_p, t_2 is the value where the pinch is formed and the emission of radiation begins but with the actual data, can't identify that moment. We only have the moment when the radial compression begins and, for small devices like the PACO this moment is close enough to the time when the pinch is formed.

Figure 4 is an example of both $V_p(t)$ and $\Delta E_p(t)$ as functions of time during the pinch stage for the same shot as before. It can be seen that ΔE_p is a continuously rising function up to a value ΔE_p^{max} while V_p passes by a maximum, V_p^{max} and later diminishes.

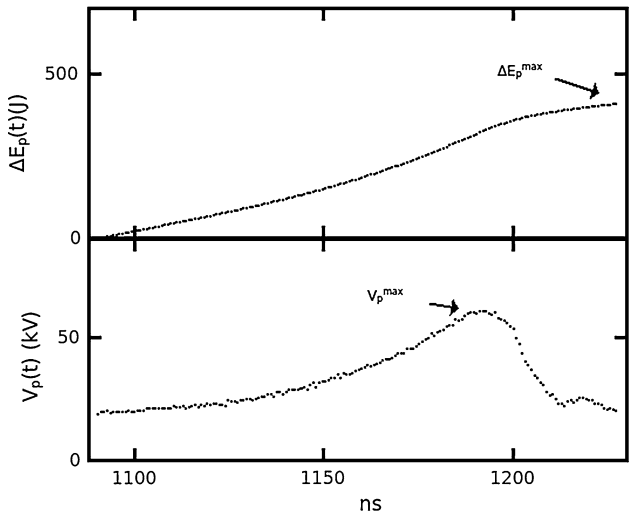

Fig. 4 Energy involved in the pinch $\Delta E_p(t)$ and voltage drop in the pinch, $V_p(t)$

Fusion Mechanisms

The scientific community agrees that the thermonuclear and the beam-target are the fundamental mechanisms in a plasma-focus device but, for each device, dominates one or a mix of both. In a previous work was discussed the fusion mechanisms [34] and here we extract the core ideas.

A thermonuclear production can be calculated as:

$$\mathrm{Y} = \frac{1}{2}\int_{\Delta t} n^2 < \sigma \mathrm{v} > \mathrm{Vol}\,\mathrm{dt}$$

where n is the deuteron density,$<\sigma v>$ is the thermal cross-section, *Vol* is the pinch volume and Δt the pinch duration.

Using the same assumptions like in the work of Moreno et al. [7], the production can be expressed as:

$$\frac{Y_n}{p_0^2} = A_1 \varepsilon^{-\frac{5}{12}} e^{\left[-\left(\frac{\varepsilon}{\varepsilon_0}\right)^{-\left(\frac{1}{3}\right)}\right]} \tag{1}$$

where ε is proportional to the Bennett temperature, p_0 is the filling pressure and A_1 is a proportionality factor.

A beam-target production can be calculated as:

$$Y_{\mathrm{bt}} \propto N_i \lambda \mathrm{n}_0$$

where N_i is the accelerated ions number, λ is the mean free path of an ion and n_0 is the plasma density.

Following the work aforementioned from Bruzzone, the production can be written as:

$$\frac{Y_n}{p_0} = A_2 e^{-\left[\frac{A_3}{V^{\frac{1}{2}}}\right]} \tag{2}$$

where A_2 and A_3 are proportionality factors and V is the voltage that accelerate the ions.

Results and Discussion

In this work, for each evaluated filling pressure, a series of 20 shots was performed. In all shots the bank energy was 1922 J (4 μF and 31 kV). To extract the results that we show here only the shots with neutron and X-ray production were selected. The complete set of filling pressures is: 0.5, 0.75, 1.0, 1.5, 2.0, 2.5, 3.0, 3.5 mbar of D_2. The better pinch production is at 1 mbar. It can be noted the narrow band of pressures where the device produces measurable radiation compared with other similar devices.

The initial inductance plus the fix inductance between the anode and the voltage divider, $L_p(0) + L'_0$, when the filling pressure changes is shown in the Fig. 5. The sum of inductances is close to 15 nH for the entire pressure range. A small decrease is noted when increasing the pressure over 1 mbar. This implicate that the current flow, when the pressure raises, takes a more distant way from the isolator (possibly an initial current sheet wider).

The current sheet lift-off is the time that the inductance reach the value *Lift-off* $[nH] = 1.1*(L_p(0) + L'_0)$. This measurement is shown in Fig. 6. At this time, the current sheet was moved from the insulator and begin the axial traveling stage. The data shown that the CS delayed when the pressure raises.

The maximum increment of energy involved in the pinch, ΔE_p^{max}, when the filling pressure changes is shown in Fig. 7. The range of energy delivered to the pinch is between 18 and 67 % of the initial capacitor bank energy. The maximum mean energy in the pinch is 37 % of the stored energy in the capacitor bank and can be found at 1 mbar diminishing at inferior and superior values.

Maximum voltage between the pinch extremes, V_p^{max}, in function of the filling pressure is shown in Fig. 8. The maximum value, 86.7 kV, was obtained at 1 mbar and the minimum was 37.5 kV. At values lower than 37.5 kV no X-ray emission was detected outside the discharge chamber. This characteristic can be understood following the Dreicer theory, previously discussed in the works of Dreicer [35, 36] and Barbaglia et al. [22, 37].

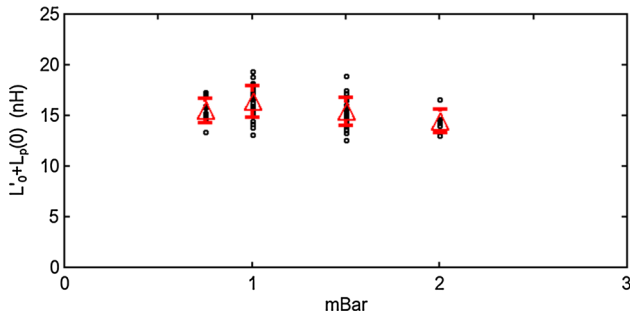

Fig. 5 The initial inductance plus the fix inductance between the anode and the voltage divider, $L_p(0) + L'_0$, in function of the filling pressure. The *small circles* are the measures and the *triangles* are the mean value of the measures

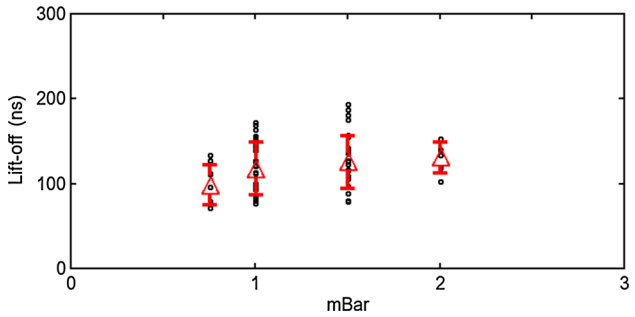

Fig. 6 Current sheet lift-off in function of the filling pressure. The *small circles* are the measures and the *triangles* are the mean value of the measures

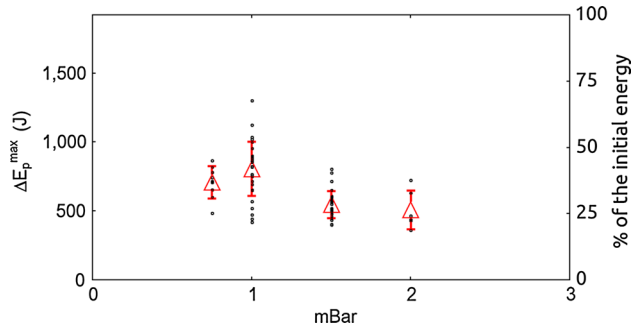

Fig. 7 Maximum increment of energy involved in the pinch, ΔE_p^{max} in function of the filling pressure. The *right vertical axis* show the percentage of the total energy system (1922 J). The *small circles* are the measures and the *triangles* are the mean value of the measures

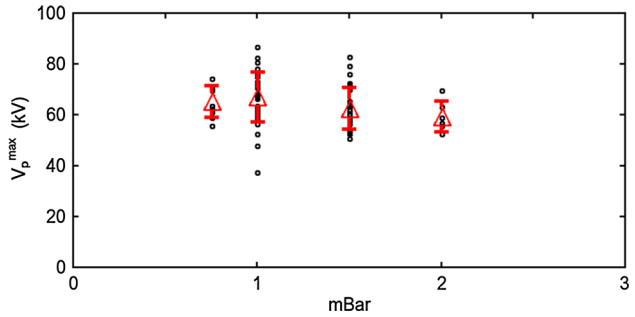

Fig. 8 Maximum voltage between the pinch extremes, V_p^{max}, in function of the filling pressure. The *small circles* are the measures and the *triangles* are the mean value of the measures

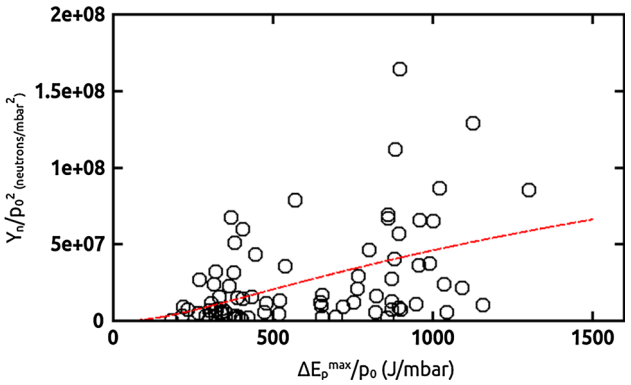

Fig. 9 Quotient between the neutronic production and the square of filling pressure, Y_n/p_0^2, in function of quotient between the increment of the energy in the pinch and the filling pressure, $\Delta E_p^{max}/p_0$. The *dashed line* is the best fit of Eq. 1 with a correlation factor of 0.19

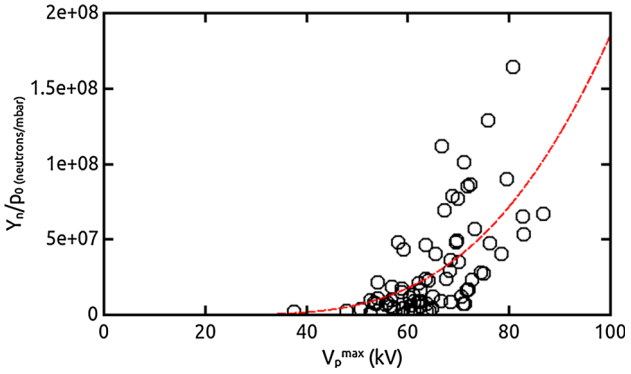

Fig. 10 Quotient between the neutronic production and the filling pressure, Y_n/p_0, in function of the maximum voltage drop in the pinch, V_p^{max}. The *dashed line* is the best fit of Eq. 2 with a correlation factor of 0.39

Figure 9 shows the quotient between the neutronic production and the square of filling pressure in function of quotient between the increment of the energy in the pinch and the filling pressure. To know the grade of correlation with the thermonuclear fusion mechanism, a fit was performed using the Eq. 1.

Assuming that in a thermonuclear system, the production by particle, Y_n/p_0^2, is a function of $\Delta E_p^{max}/p_0$, the best fit is (dashed curve in the figure):

$$\frac{Y_n}{p_0^2} = 5.54 \cdot 10^{10} \left(\frac{\Delta E_p^{max}}{p_0}\right)^{-\frac{5}{12}} e^{\left[-\left(\frac{\left(\frac{\Delta E_p^{max}}{p_0}\right)}{74934}\right)^{-\left(\frac{1}{3}\right)}\right]}$$

with a correlation factor of 0.19.

Figure 10 shows the quotient between the neutronic production and the filling pressure in function of the maximum voltage drop in the pinch. If the fusion mechanism is beam-target, the data need to fit with the Eq. 2. The best fit is (dashed curve in the figure):

$$\frac{Y_n}{p_0} = 5.7 \cdot 10^{11} e^{-\left[\frac{2.54 \cdot 10^3}{\left(V_p^{max}\right)^{\frac{1}{2}}}\right]}$$

with a correlation factor of 0.39.

Conclusions

The presented method of analysis is a simple tool to reveal the behaviors of the plasma focus machine. The data reported show a scenario where the CS increases its size and the lift-off is slower when the filling pressure rises. The best efficiency to produce radiation can be found at 1 mbar. Considering that the hard X-ray coming of an electron runaway and posterior Bremsstrahlung mechanism, the X-ray produced has a limit in the higher voltage between the pinch extremes, 86 keV. The maximum mean energy transferred into the pinch is 37 % of the stored energy in the capacitor bank, and the peak maximum transfer of energy is close to 67 % from the initial system energy with a cost of 7 μJ for each neutron produced.

Taking into account the approximation performed and the fitting results, the fusion mechanism, probably, is a mix between thermonuclear and beam-target. This interesting result, contrast with the reported by Bruzzone et al. [34] where was studied the same device, but with a different cathode type.

Acknowledgments This research was supported in part by the Fund for Scientific Research and Technology (FONCyT) PICT 2012 N° 0926, the National Scientific and Technical Research Council (CONICET) of Argentina PIP 0391 and by the National University of the Center of the Buenos Aires Province (UNCPBA). C. Pavez, J. Moreno and L. Soto from Chile supported by CONICYT-PIA grant ACT-1115. M. Barbaglia thanks to the Argentina National Atomic Energy Commission (CNEA) and International Atomic Energy Agency (IAEA) for support to spread this knowledge.

References

1. J.W. Mather, Phys. Fluids **8**(366), 1958–1988 (1965)
2. J.W. Mather, Phys. Fluids **7**(S28), 1958–1988 (1964)
3. N.V. Filippov, T.I. Filippova, V.P. Vinogradov, Nucl. Fusion Suppl. **2**, 577 (1962)
4. H. Bruzzone, R. Vieytes, Plasma Phys. Control. Fusion **35**, 1745 (1993)
5. L. Soto, Plasma Phys. Control. Fusion **47**, A361 (2005)
6. P. Kubes, D. Klir, M. Paduch, T. Pisarczyk, M. Scholz, T. Chodukowski, Z. Kalinowska, K. Rezac, J. Kravarik, J. Hitschfel, J. Kortanek, B. Bienkowska, I. Ivanova-Stanik, L. Karpinski, M.J. Sadowski, K. Tomaszewski, E. Zielinska, I.E.E.E. Trans, Plasma Sci. **40**, 1075 (2012)
7. C. Moreno, H. Bruzzone, J. Martínez, A. Clausse, IEEE Trans. Plasma Sci. **28**, 1735 (2000)
8. S. Lee, J. Fusion Energ. **33**, 319 (2014)

9. M. Milanese, O.D. Cortazar, R. Moroso, J. Niedbalski, J.L. Supan, I.E.E.E. Trans, Plasma Sci. **39**, 2402 (2011)
10. A. Patran, D. Stoenescu, R.S. Rawat, S.V. Springham, T.L. Tan, L.C. Tan, M.S. Rafique, P. Lee, S. Lee, J. Fusion Energ. **25**, 57 (2006)
11. M. Zakaullah, I. Ahmad, A. Omar, G. Murtaza, M.M. Beg, Plasma Sources Sci. Technol. **5**, 544 (1996)
12. V.I. Krauz, Plasma Phys. Control. Fusion **48**, B221 (2006)
13. M.A. Tafreshi, M.M. Nasseri, N. Nabipour, D. Rostamifard, A. Nasiri, J. Fusion Energ. **33**, 689 (2014)
14. C. Moreno, M. Vénere, R. Barbuzza, M. Del Fresno, R. Ramos, H. Bruzzone, F.P.J. González, A. Clausse, Braz. J. Phys. **32**, 20 (2002)
15. F. Castillo, I. Gamboa-deBuen, J.J.E. Herrera, J. Rangel, S. Villalobos, Appl. Phys. Lett. **92**, 051502 (2008)
16. A. Fabbri, M. Frignani, S. Mannucci, D. Mostacci, F. Rocchi, M. Sumini, F. Teodori, E. Angeli, A. Tartari, G. Cucchi, J. Radiol. Prot. **27**, 465 (2007)
17. R.S. Rawat, T. Zhang, K.S.T. Gan, P. Lee, R.V. Ramanujan, Appl. Surf. Sci. **253**, 1611 (2006)
18. M. Krishnan, I.E.E.E. Trans, Plasma Sci. **40**, 3189 (2012)
19. V.D. Aleksandrov, E.P. Bogolubov, O.V. Bochkarev, L.A. Korytko, V.I. Nazarov, Y.G. Polkanov, V.I. Ryzhkov, T.O. Khasaev, Appl. Radiat. Isot. **63**, 537 (2005)
20. W. Rogowski, W. Steinhaus, Arch. Elektrotech. **1**, 141 (1912)
21. Z.Y. Lee, Rev. Sci. Instrum. **54**, 1060 (1983)
22. M. Barbaglia, L. Soto, A. Clausse, J. Fusion Energ. **31**, 105 (2011)
23. P. Kubes, M. Paduch, T. Pisarczyk, M. Scholz, T. Chodukowski, D. Klir, J. Kravarik, K. Rezac, I. Ivanova-Stanik, L. Karpinski, K. Tomaszewski, E. Zielinska, I.E.E.E. Trans, Plasma Sci. **37**, 2191 (2009)
24. F. Castillo, J.J.E. Herrera, J. Rangel, M. Milanese, R. Moroso, J. Pouzo, J.I. Golzarri, G. Espinosa, Plasma Phys. Control. Fusion **45**, 289 (2003)
25. J. Moreno, L. Birstein, R.E. Mayer, P. Silva, L. Soto, Meas. Sci. Technol. **19**, 087002 (2008)
26. V. Raspa, C. Moreno, L. Sigaut, A. Clausse, Phys. Scr. **T131**, 014034 (2008)
27. H. Kelly, A. Marquez, Meas. Sci. Technol. **6**, 400 (1995)
28. M.M. Milanese, O.D. Cortázar, M.O. Barbaglia, R.L. Moroso, I.E.E.E. Trans, Plasma Sci. **42**, 2606 (2014)
29. M.J. Bernstein, Rev. Sci. Instrum. **41**, 1843 (1970)
30. H. Bruzzone, H. Acuña, M. Barbaglia, A. Clausse, Plasma Phys. Control. Fusion **48**, 609 (2006)
31. P.G. Eltgroth, Phys. Fluids **25**(2408), 1958–1988 (1982)
32. H. Bruzzone, H. Acuna, A. Clausse, Plasma Phys. Control. Fusion **49**, 105 (2007)
33. H. Bruzzone, H. Acuña, A. Clausse, Braz. J. Phys. **38**, 117 (2008)
34. H. Bruzzone, M.O. Barbaglia, H. Nestor Acuna, M.M. Milanese, R.L. Moroso, S. Guichon, IEEE Trans. Plasma Sci. **41**, 3180 (2013)
35. H. Dreicer, Phys. Rev. **115**, 238 (1959)
36. H. Dreicer, Phys. Rev. **117**, 329 (1960)
37. M. Barbaglia, H. Bruzzone, H. Acuña, L. Soto, A. Clausse, Plasma Phys. Control. Fusion **51**, 045001 (2009)